Developmental Cell
Article

Feedback Inhibition of JAK/STAT Signaling by Apontic Is Required to Limit an Invasive Cell Population

Michelle Starz-Gaiano,[1,3] Mariana Melani,[1,3] Xiaobo Wang,[1] Hans Meinhardt,[2] and Denise J. Montell[1,*]
[1]Department of Biological Chemistry, Johns Hopkins University School of Medicine, 855 North Wolfe Street, Baltimore, MD 21205, USA
[2]Max-Planck-Institut für Entwicklungsbiologie, Spemannstrasse 35, D-72076 Tübingen, Germany
[3]These authors contributed equally to this work.
*Correspondence: dmontell@jhmi.edu
DOI 10.1016/j.devcel.2008.03.005

SUMMARY

In both normal development and in a variety of pathological conditions, epithelial cells can acquire migratory and invasive properties. Border cells in the *Drosophila* ovary provide a genetically tractable model for elucidating the mechanisms controlling such behaviors. Here we report the identification of a mutant, *apontic (apt)*, in which the migratory population expanded and separation from the epithelium was impeded. This phenotype resembled gain-of-function of JAK/STAT activity. Gain-of-function of APT also mimicked loss of function of STAT and its key downstream target, SLBO. APT expression was induced by STAT, which bound directly to sites in the *apt* gene. The data suggest that a regulatory circuit between STAT, APT, and SLBO functions to convert an initially graded signal into an all-or-nothing activation of JAK/STAT and thus to proper cell specification and migration. These findings are supported by a mathematical model, which accurately simulates wild-type and mutant phenotypes.

INTRODUCTION

In a variety of biological contexts, epithelial cells can acquire the ability to migrate. This occurs repeatedly during embryonic development and is presumed to occur when carcinoma cells metastasize. For cells to migrate out of an epithelium, they must gain a number of properties that distinguish them from the cells that stay behind. They have to become competent to extend protrusions, and importantly, they must detach from their neighbors. In vivo, this transformation requires changes in gene expression; however, the molecular mechanisms that govern these events are incompletely understood. For example, it is not clear how the ability to move is restricted to the appropriate subset of cells during development or how, in metastasis, cells newly acquire the capacity to break away from the primary tumor.

Border cells in the *Drosophila* ovary provide a genetically tractable model to study the specification of a migratory population. Border cells form within the follicle cell epithelium, detach from it, and migrate to the oocyte (reviewed in Jang et al., 2007; Montell, 2006). The egg chamber is the functional unit of the fly ovary and is composed of an oocyte, 15 nurse cells, and a surrounding epithelium composed of about 650 follicle cells (Figure 1). Oogenesis can be subdivided into 14 stages (King, 1970). Early on, a specialized pair of cells, known as polar cells, arises at each end of the egg chamber. At stage 8, the polar cell pair secretes a cytokine that specifies the surrounding cells to become border cells at the anterior. At stage 9, border cells round up and adhere to the polar cells as they exit the epithelium, migrate 150–200 microns, and reach the oocyte border by stage 10 (Figures 1A–1C). Ultimately, these cells produce a structure called the micropyle, which is required for fertilization.

The JAK/STAT signaling pathway is critical for normal embryonic development and immune system function in flies as well as in mammals. Previous work has shown that JAK/STAT signaling is essential for specification and migration of the border cells (Arbouzova and Zeidler, 2006; Beccari et al., 2002; Ghiglione et al., 2002; Silver et al., 2005; Silver and Montell, 2001; Xi et al., 2003). Polar cells secrete the cytokine Unpaired (Upd), which activates a receptor known as Domeless (DOME) in the surrounding cells. Ligand binding to DOME activates the associated Janus Kinase (JAK), which phosphorylates DOME, leading to recruitment and phosphorylation of STAT. STAT then dimerizes and translocates to the nucleus where it activates transcription of target genes. Although UPD is diffusible and DOME is expressed in all follicle cells, the 4–8 cells directly contacting the anterior polar cells exhibit the highest level of STAT activation and typically only those become border cells, while the remaining anterior cells develop into squamous nurse cell-associated follicle cells (Beccari et al., 2002; Ghiglione et al., 2002; Silver and Montell, 2001; Xi et al., 2003).

A precise level of JAK/STAT activity must be achieved for the correct specification and migration of the border cell population. Ectopic JAK/STAT signaling results in the migration of additional border cells (Silver and Montell, 2001). A key downstream target of STAT is the *slow border cells* (*slbo)* gene, which is a basic region and leucine zipper-containing transcription factor related to mammalian C/EBPs (Montell et al., 1992). Either inadequate or excess SLBO protein can inhibit migration, reducing fertility (Montell et al., 1992; Rorth et al., 2000). However, the mechanisms that limit JAK/STAT signaling and SLBO expression to the appropriate number of cells and to the optimal level are not clear. Here we report genetic, cell biological,

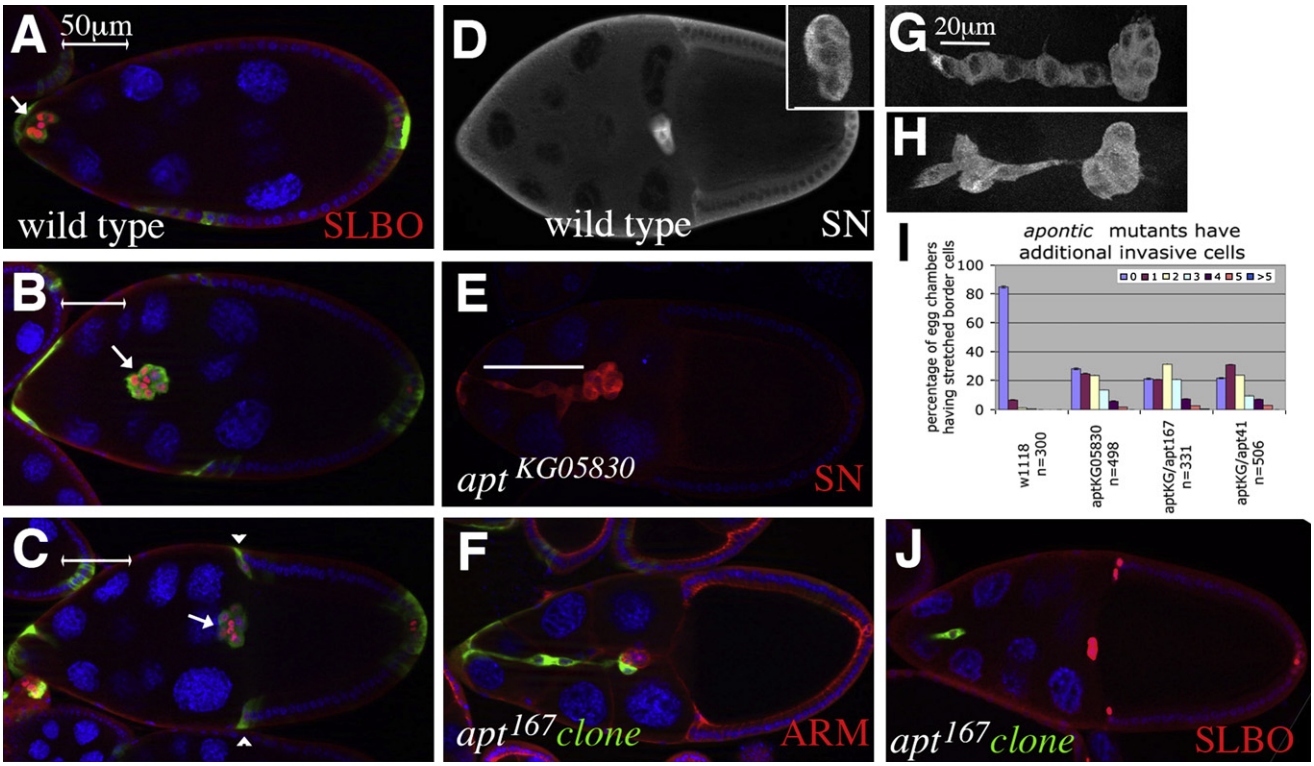

Figure 1. *apt* Is Required Cell Autonomously to Limit Follicle Cell Invasion

(A–C) Wild-type border cell migration. *slbo-Gal4, UAS-mCD8-GFP* egg chambers stained with antibodies against GFP (green) and SLBO (red), and DAPI (blue) to label all nuclei. Anterior is to the left. The scale bar indicates 50 μm.

(A) A stage 9 egg chamber. The border cells (arrow) detach from the follicular epithelium and start migrating.

(B) At mid-stage 9, the border cell cluster (arrow) has migrated 50% of the distance to the oocyte.

(C) A stage 10 egg chamber, the border cells (arrow) are at the oocyte border. Centripetal cells (arrowheads) will begin migrating inward.

(D and E) Stage 10 egg chambers stained with anti-Singed antibody shows the morphology of the border cells.

(D) Control stage 10 egg chamber. The border cell cluster has reached the oocyte as a unit (magnified in inset).

(E–H) *apt* affects border cell number and cluster morphology.

(E) Stage 10 $apt^{KG05830}$ egg chamber. Five extra SN-expressing cells (bracket) moved between the nurse cells behind the main border cell cluster but were still connected to the outer follicle cell epithelium.

(F) Positively-marked apt^{167} clone stained with DAPI (blue) and antibodies against ARM (red) and GFP (green). Homozygous mutant cells (green) include one at the anterior tip of the egg chamber, several stretched border cells, and one within the border cell cluster.

(G and H) High magnification of $apt^{KG05830}/apt^{KG05830}$ (G) and $apt^{KG05830}/apt^{41}$ (H) border cell clusters stained with SN antibody. Scale bar is 20 μm. Five lagging cells (stretched border cells) and their abnormal morphology can be appreciated (compare with inset in [D]).

(I) Number of additional invasive cells in various *apt* allelic combinations. Error bars represent one standard error.

(J) Positively-marked apt^{167} single mutant stretched border cell (green) indicates that the phenotype is cell autonomous.

and biochemical evidence that the *apt* gene plays a critical role in this process as a feedback inhibitor of STAT and SLBO, a conclusion that is further supported by mathematical modeling.

RESULTS

A Novel Allele of *apt* Affects Border Cell Development

In order to identify new genes that play a role in border cells, we screened 2951 homozygous-viable P element insertions (Bellen et al., 2004) for a loss-of-function effect on border cells. We found one line, P{SUPor-P}^{KG05830}, with a unique phenotype. In 75% of stage 10 egg chambers, we observed 1–7 additional invasive cells, often dramatically stretched out and trailing behind the main cluster (Figures 1E–1I), compared to wild-type (Figures 1A–1D). In addition, in about 32% of stage 10 P{SUPor-P}^{KG05830} egg chambers, the cells failed to complete their migration to the oocyte (Figure S1A, see the Supplemental Data available with this article online).

P{SUPor-P}^{KG05830} contains a transposon insertion in the *apt* gene (Figure S1B), also known as *tracheal defective* (*tdf*, Eulenberg and Schuh, 1997; Gellon et al., 1997; Lie and Macdonald, 1999; Su et al., 1999). Complementation tests with existing *apt* alleles showed that P{SUPor-P}^{KG05830} is a novel, viable allele (Figure 1I and Figure S1A), which we will refer to as $apt^{KG05830}$. The strongest defects were observed in combination with apt^{167}, apt^{41}, or a deficiency for the locus (Figure 1I and Figure S1A). In these genotypes, 80% of egg chambers had additional, invasive cells positive for known border cell markers, including Singed (Figures 1G and 1H) and SLBO proteins (Figure 2I, Montell et al., 1992). We will refer to these cells as "stretched border cells."

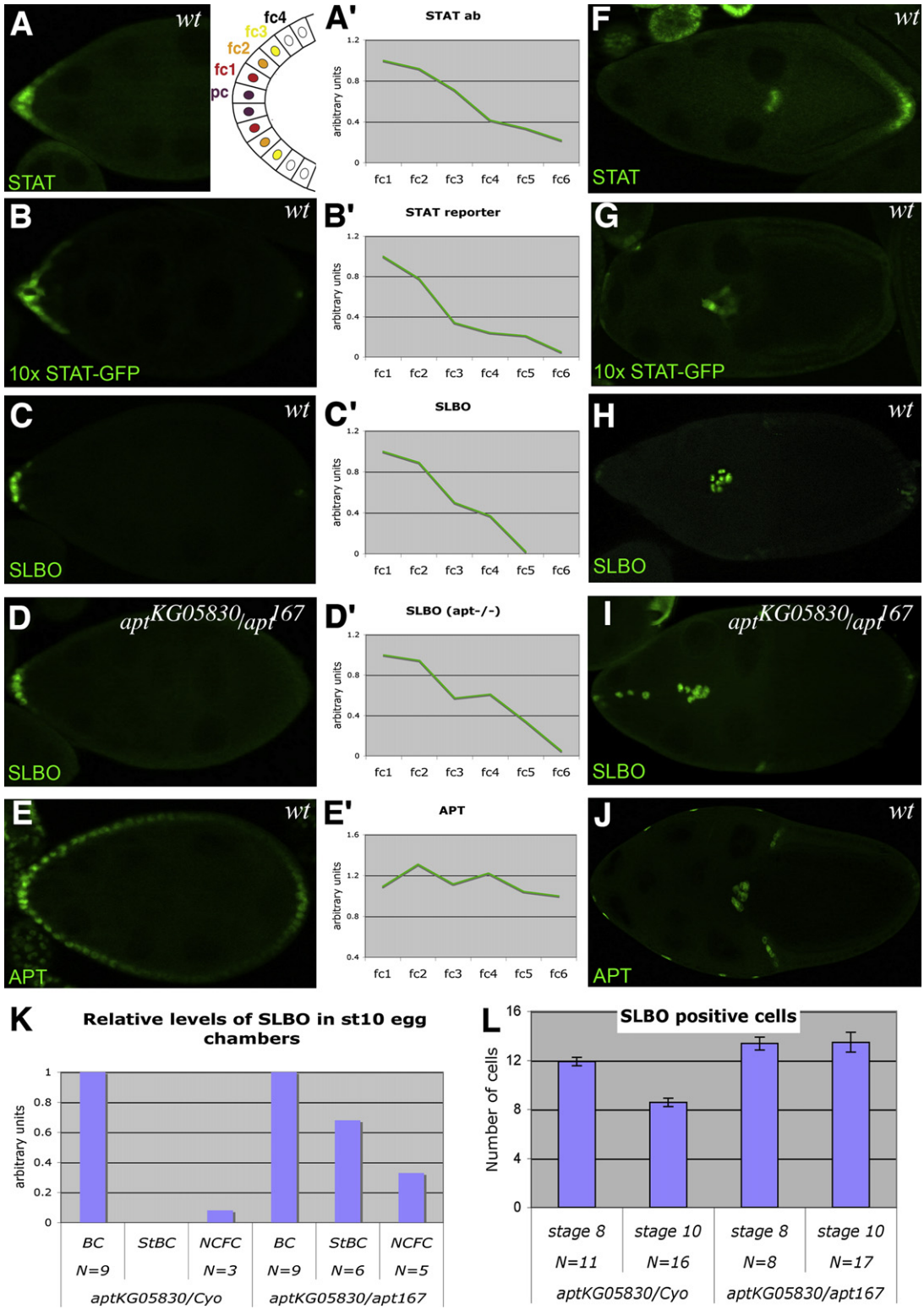

Figure 2. Expression of STAT Targets

Immunofluorescence micrographs of stage 8 (A–E) and late stage 9 or stage 10 egg chambers (F–J) stained to detect expression of the indicated STAT targets, including STAT itself.

(A′–E′) Relative levels of nuclear staining intensity of each of the STAT targets relative to DAPI staining intensity plotted as a function of distance from the polar cells. Fc1 indicates the cell next to the polar cell, fc2 the next cell, and so on, as shown in the diagram in panel A. n > 3 for each data point. All egg chambers are wild-type except for (D) and (I) which are homozygous for $apt^{KG05830}$.

We used mosaic analysis to determine in which cell type(s) *apt* is required. Egg chambers containing clones of cells homozygous for apt^{167}, apt^{41}, or $apt^{P\Delta 3}$ exhibited defects like those observed in the viable $apt^{KG05830}$ mutant flies (Figures 1F and 1J and data not shown). Interestingly, even when only one or a few anterior follicle cells were mutant, identified by expression of GFP in MARCM clones (Lee and Luo, 1999), we could see trailing stretched border cells (Figures 1F and 1J). In contrast, we did not observe any stretched border cell that was wild-type in genotype in more than 100 egg chambers containing *apt* clones. We also did not observe a phenotype when only border cells were mutant. Together these findings indicate that *apt* is normally required autonomously in cells adjacent to the border cells to prevent their invasion and to promote detachment of the migrating cells from those that remain within the epithelium.

APT is highly conserved in fly and mosquito species, and contains a predicted Myb/SANT motif (Figures S1C and S1D), which is a DNA binding domain, and previous work has shown that APT can bind to DNA (Liu et al., 2003). The closest protein to APT in humans is Fibrinogen silencer-binding protein (FSBP, Mizuguchi et al., 1995). FSBP contains a region that is 23% identical and 45% similar to APT over 97 amino acids (Figure S1C). The EMS-induced allele apt^{167}, which behaves genetically as a null allele, and apt^{41}, a strong loss-of-function allele, are missense mutations in arginine residues within this region that are conserved in all species analyzed. The FSBP gene is very well conserved throughout mammals, and it has been described as a negative regulator of the transcription of the gamma chain of *fibrinogen* (Mizuguchi et al., 1995). APT and the mammalian proteins also contain two predicted coiled-coil motifs (Figure S1D).

APT Affects JAK/STAT Signaling

Although unique among loss-of-function mutant phenotypes, the presence of extra invasive cells resembled gain-of-function of the JAK/STAT pathway in anterior follicle cells (Silver et al., 2005). This suggested that APT might antagonize JAK/STAT. To understand better how the additional border cells were specified in *apt* mutants, we carefully examined JAK/STAT activation in wild-type and *apt* mutant egg chambers. We used several known markers of JAK/STAT activation including STAT itself (Xi et al., 2003), a STAT-responsive reporter (STAT-GFP, Bach et al., 2007), and SLBO (Silver and Montell, 2001). In wild-type egg chambers at stage 8, STAT accumulated in the nuclei of anterior follicle cells in a graded manner (Figures 2A and 2A′). We quantified the level of nuclear STAT expression relative to DAPI staining intensity as a function of cell position (distance from polar cells) and found that STAT was activated to highest levels in the cells adjacent to the polar cells (fc1, Figures 2A and 2A′). The level of activation was slightly lower in the next cell over (fc2), fell precipitously in the third cell from the polar cell (fc3), and continued to decline with increasing distance from the source of the activating ligand. Similar patterns were also apparent for the STAT-GFP reporter and the known STAT target SLBO (Figures 2B–2C′) and are consistent with previous reports of a gradient of STAT activity (Devergne et al., 2007; Xi et al., 2003).

By late stage 9, these gradients had changed. STAT itself, STAT-GFP, and SLBO continued to be highly expressed in border cells (and cells adjacent to posterior polar cells), but not in other anterior follicle cell types (Figures 2F–2H). Therefore the initially graded STAT response evolved into a step function with "on" and "off" states.

In *apt* mutants, at stage 8, the gradient of SLBO was similar to wild-type (Figure 2D). However at stages 9 and 10, SLBO levels in the stretched border cells were intermediate between those in the clustered border cells and those in the nurse cell-associated follicle cells (compare Figures 2H and 2I). Therefore SLBO expression remained graded in *apt* mutants instead of evolving to a step function as in wild-type (Figure 1K).

In control egg chambers SLBO expression was detected in 12 anterior follicle cells at stage 8 (Figure 2L). Similar numbers of cells were SLBO-positive in homozygous $apt^{KG05830}$ or $apt^{KG05830}/apt^{167}$ egg chambers at this stage (Figures 2D and 2L). As oogenesis progressed, the number of cells detectably expressing SLBO was normally reduced to an average of eight cells, which were the cells of the migrating cluster (Figure 2L). In contrast, in *apt* mutant egg chambers, no decline in the number of SLBO-positive cells was observed (Figures 2I and 2L). As a result, an average of 13 SLBO positive cells could be identified both at stage 8 and at stage 10. This demonstrates that cells that normally turn SLBO expression off in wild-type controls retain SLBO expression in *apt* mutants.

APT Expression Is Regulated by the STAT Pathway

We next investigated APT expression and its regulation during egg chamber development. Throughout stages 8–10, the highest levels of expression were observed in the border cells and the anterior nurse cell-associated follicle cells and in a few posterior follicle cells (Figures 2E, 2E′, and 2J, and Figure S2A–S2D′). APT protein levels were dramatically reduced in anterior follicle cells of $apt^{KG05830}$ mutant egg chambers (Figures S2E and S2F).

apt has been reported to be a downstream transcriptional target of STAT in the testis (Terry et al., 2006). In addition, in a microarray analysis of purified border cells, *apt* expression was upregulated in response to overexpression of UPD, relative to wild-type (X.W. and D.J.M., unpublished data). To investigate further if APT is a STAT target in follicle cells, we induced homozygous mutant clones and found that *stat* mutant border cells expressed a level of APT that was 66% of that of heterozygous cells in the same cluster (Figures 3A–3A″). We then tested whether ectopic activation of the JAK/STAT pathway could induce ectopic expression of APT. Using the FLP-out technique, a constitutively active form of JAK (hop^{Tum}) was expressed in random clones to activate the STAT pathway. In oocyte-associated outer follicle cells, which normally do not express APT, it was induced in response to hop^{Tum} (Figures 3B–3B‴). Strikingly, the level of APT

(K) Quantification of the level of SLBO expression, relative to DAPI staining in border cells (BC), stretched border cells (StBC), and nurse cell associated follicle cells (NCFC) in heterozygous and homozygous *apt* egg chambers.

(L) Quantification of border cell number in heterozygous and homozygous *apt* egg chambers. Error bars represent one standard error. Note a significant difference between the number of SLBO positive cells at stage 8 and 10 in wild-type controls ($p < 0.001$).

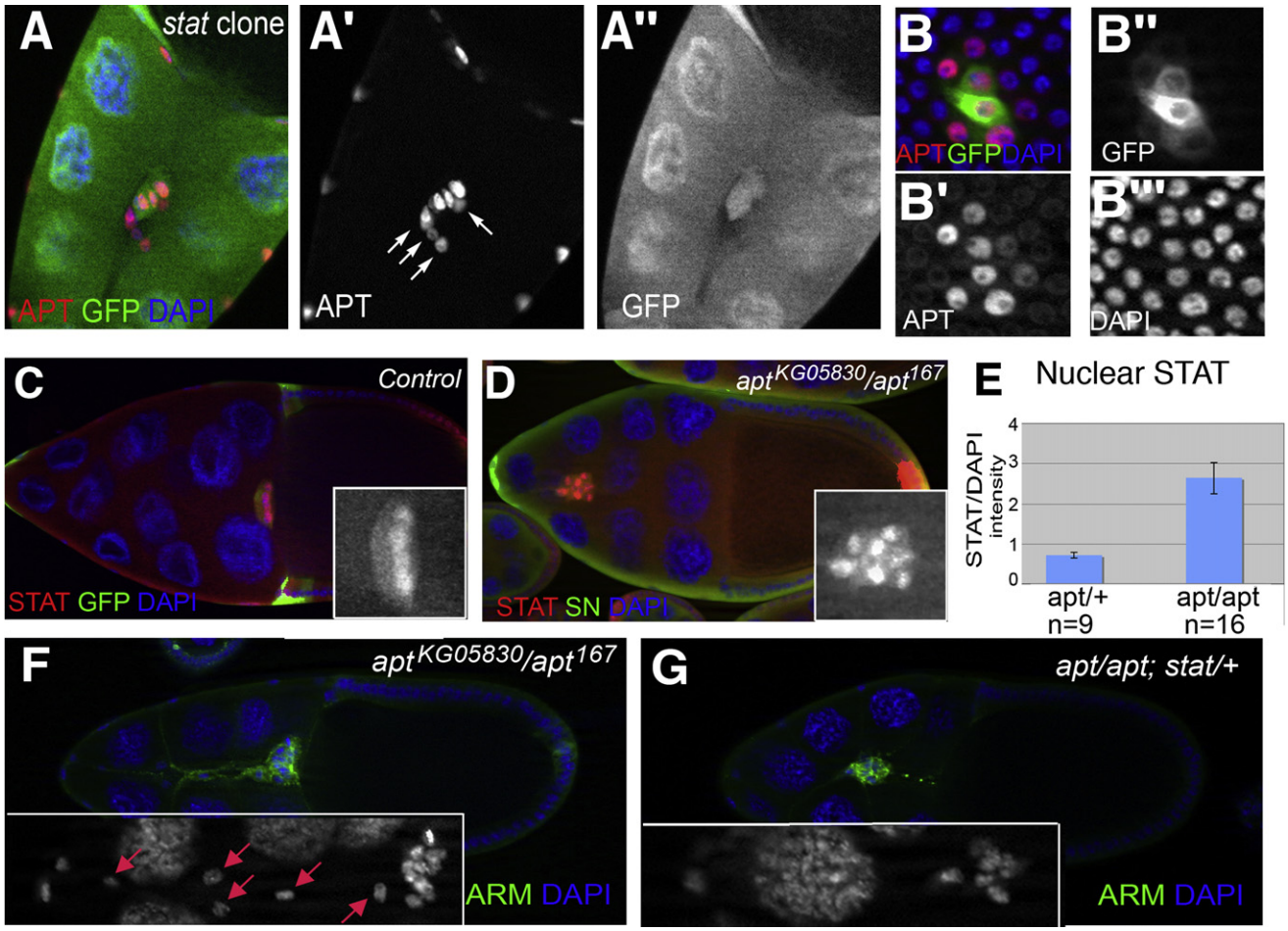

Figure 3. Apontic Is a Target and a Negative Regulator of STAT Signaling

(A–A″) *stat* loss-of-function affects APT expression. A late stage 10 egg chamber containing a border cell cluster composed of a mixture of wild-type (GFP-positive) and *stat* mutant (GFP-negative, arrows) cells stained for APT (red in [A], white in [A′]).

(B–B‴) Ectopic STAT activation affects APT expression. Oocyte-associated follicle cells containing a clone of cells expressing GFP and HOP^{TUM}, stained for APT and DAPI. Overlay is shown in (B).

(C–E) STAT activation is affected by *apt*. Control (C) or *apt* mutant (D) stage 10 egg chambers stained for the indicated markers. Insets, STAT antibody.

(E) Quantification of the ratio of STAT nuclear staining to DAPI intensity for border cells of the indicated genotypes. Error bars show one standard error.

(F and G) Genetic interaction between *apt* and *stat*. In $apt^{KG05830}/apt^{167}$ egg chambers (F), stretched border cells trail behind the main cluster (red arrows in DAPI inset). In $apt^{KG05830}/apt^{167}$; $stat^{1681}$/+ egg chambers (G), there is a significant reduction in the number of stretched border cells.

that was induced was similar in cells that expressed different amounts of hop^{Tum}. This observation suggested that the transcriptional effect of STAT on APT saturates at relatively low levels of STAT activation, which is consistent with the relatively uniform expression of APT that we observed across the anterior follicular epithelium despite the graded activation of STAT (Figures 2E and 2E′).

APT Limits STAT Signaling and Border Cell Recruitment

Overexpression of activated JAK (hop^{Tum}) in anterior follicle cells leads to extra cells that trail behind the main border cell cluster (Silver et al., 2005). Given the similarity between this phenotype and that seen in *apt* mutants, and the induction of APT expression by STAT, we hypothesized that APT may function as a feedback inhibitor to restrict the highest levels of JAK/STAT signaling to the cells adjacent to the polar cells. To investigate this, we examined the level of STAT nuclear accumulation as a measure of STAT pathway activity, in wild-type and *apt* mutant border cells (Figures 3C–3E). In *apt* mutants, the ratio of STAT staining to DAPI staining was 3-fold higher than the ratio in control border cells (Figure 3E).

We then tested for a genetic interaction between *apt* and *stat*. In $apt^{KG05830}/apt^{167}$; $stat^{1681}$/+ egg chambers, we saw a reduction in the frequency and number of stretched border cells compared to mutants homozygous for *apt* alone (Figures 3F and 3G). On average, 26% of $apt^{KG05830}/apt^{167}$; $stat^{1681}$/+ egg chambers had stretched border cells, compared to 80% in $apt^{KG05830}/apt^{167}$; + /TM6 sibling controls. Moreover, the border cell cluster clearly detached from the anterior end much more frequently when the *apt* mutants were also heterozygous for *stat,* consistent with the idea that reduction in *stat* expression ameliorated the *apt* phenotype.

Functional Antagonism between *apt* and *slbo*

In addition to the loss-of-function phenotype, *apt* exhibited a severe gain-of-function phenotype when overexpressed in border cells. We used the Gal4/UAS system to overexpress an isoform of *apt* (UAS-*tdf*, the RC isoform, Eulenberg and Schuh, 1997) specifically in the border cells under the control of *slbo*-Gal4. High levels of APT resulted in a complete failure of border cell movement (Figure 4A). Some cells clustered around the polar cells; however, they never managed to leave the follicular epithelium or invade in between the nurse cells. A key downstream target of STAT in border cells is the *slbo* gene (Silver and Montell, 2001), which encodes a basic region and leucine zipper-containing transcription factor of the C/EBP family. The severe border cell migration defect observed following APT overexpression in border cells resembles the *slbo* loss of function phenotype (Figure 4B). Consistent with this observation, overexpression of *slbo* remarkably resembles *apt* loss-of-function and results in the presence of stretched border cells (Figures 4C and 4D). Therefore, we examined expression of SLBO in border cells with higher than wild-type levels of APT (Figures 4E, 4F, 4J, and 4K). Whereas all eight cells including the polar cells in a wild-type cluster express SLBO, only two to four cells expressed detectable SLBO following APT overexpression using the *slbo-Gal4* driver (Figures 4F, 4J, and 4K), two of which are likely the polar cells, which do not express the driver (Geisbrecht and Montell, 2002). Thus, APT negatively affects *slbo* gene expression. Overexpression of SLBO also inhibits APT expression, though to a lesser degree (Figures 4D and 4G–4I). Whereas APT protein is evenly expressed in all cells, including polar cells, of a wild-type cluster (Figure 4G), overexpression of *slbo* using *slbo-Gal4* leads to a lower level of APT expression in the outer cells compared to the central polar cells, which do not express the *Gal4* driver (Figure 4I). Conversely, elevated APT expression is observed in *slbo* mutant border cells (Figure 4H). Consistent with this observation, we detected upregulation of *apt* mRNA in *slbo* mutant border cells compared to wild-type in a microarray analysis (X.W. and D.J.M., unpublished data).

Previously, APT had been described both as a DNA binding protein and as a translational regulator (Eulenberg and Schuh, 1997; Gellon et al., 1997; Lie and Macdonald, 1999; Liu et al., 2003; Su et al., 1999). To test whether APT affects *slbo* at the level of transcription, we overexpressed *apt* in the background of the $slbo^{1310}$ enhancer trap. In this line, a P element containing a minimal promoter and the *lacZ* gene is inserted between the border cell enhancer of the *slbo* locus and the start site of transcription (Montell et al., 1992). In egg chambers of the $slbo^{1310}$ enhancer trap, β-galactosidase is strongly expressed in the border cell cluster, including both the outer migratory border cells and the nonmotile polar cells (Montell et al., 1992; Figure 4L). Overexpression of *apt* using *slbo-Gal4* caused a dramatic reduction in β-galactosidase activity in the border cells but not in the polar cells (Figure 4M), demonstrating that APT transcriptionally affects the *slbo* locus. This is consistent with the loss-of-function data for *apt*, in which more cells express SLBO than wild-type (Figure 2I).

Given the opposing phenotypes of *apt* and *slbo*, both with respect to loss- and gain-of-function, we tested whether overexpression of the two genes together could result in a rescue of the border cell defects. To do this, we coexpressed both genes in the border cells using the *slbo-Gal4* driver. Overexpression of both APT and SLBO ameliorated defects in border cell cluster detachment from the epithelium (Figure 4N) that were seen when APT was overexpressed alone (Figures 4A, 4F, and 4O) or in combination with UAS-GFP or UAS-LacZ (Figure 4O). Whereas SLBO overexpression alone generated many additional stretched border cells (Figure 4D), these extra invasive cells were almost never seen in the double overexpression cases (Figures 4N and 4O).

Live Imaging Confirms Delayed Detachment in *apt* Loss of Function and *slbo* Overexpression

The observation that *apt* mutant stretched border cells frequently fail to detach from the border cell cluster and/or the anterior follicle epithelium led us to examine the detachment step more carefully in wild-type. While it takes approximately six hours from the time the border cells begin extending protrusions until they reach the oocyte (Prasad and Montell, 2007), about 1/3 of that time is spent separating from the epithelium (Movie S1). The follicle cells from which the border cells detach stretch toward each other, maintaining the continuity of the epithelium while the border cell cluster moves away (Movie S2).

To compare the *apt* loss-of-function and *slbo* overexpression phenotypes by live imaging, we crossed *slbo-Gal4*; UAS-mCD8GFP into these backgrounds (Figure S3 and Movies S3 and S4). In both genotypes, we observed that the main border cell cluster formed and initiated migration normally, but that as it moved it remained tethered to the follicular epithelium by one or more cells. As the cluster moved away from the anterior end of the egg chamber, the attached cells also invaded into the germ line tissue. In the *slbo* overexpression case, as the main cluster migrated toward the oocyte, it remained attached to the lagging cells, and those cells remained connected to the anterior tip of the egg chamber (Figure S3C and Movie S3). In *apt* mutants, the majority of border cell clusters eventually detached (Movie S4) but were delayed in this step relative to wild-type (Figures S3B and S3D). We assessed when the border cells severed their connection with the anterior follicle cells relative to the onset of *slbo-Gal4*-mediated expression of mCD8GFP in the future centripetal follicle cells (Figure S3A–S3D). In wild-type egg chambers, border cells detached on average 4.6 min prior to the onset of GFP expression in the centripetal cells (n = 6), although there was significant variability (Figure S3D). In *apt* mutant egg chambers, detachment occurred on average 83 min later, confirming a significant delay. This may account for the observation that in some *apt* mutant egg chambers, border cells failed to reach the oocyte on time even when stretched border cells were not evident (Figure S3E–S3H).

Mechanism of APT Action

To determine whether STAT and APT bind directly to *slbo* gene regulatory sequences, we first inspected them for likely STAT and APT binding sites. We focused on a 3.2 kb fragment of *slbo* genomic DNA known to reproduce the normal *slbo* expression pattern in follicle cells when fused to Gal4 or GFP-actin (Fulga and Rorth, 2002; Rorth, 1994). We identified five putative STAT binding sequences and three potential APT binding sites (Figure 5A). To test for STAT binding, we first labeled an optimal

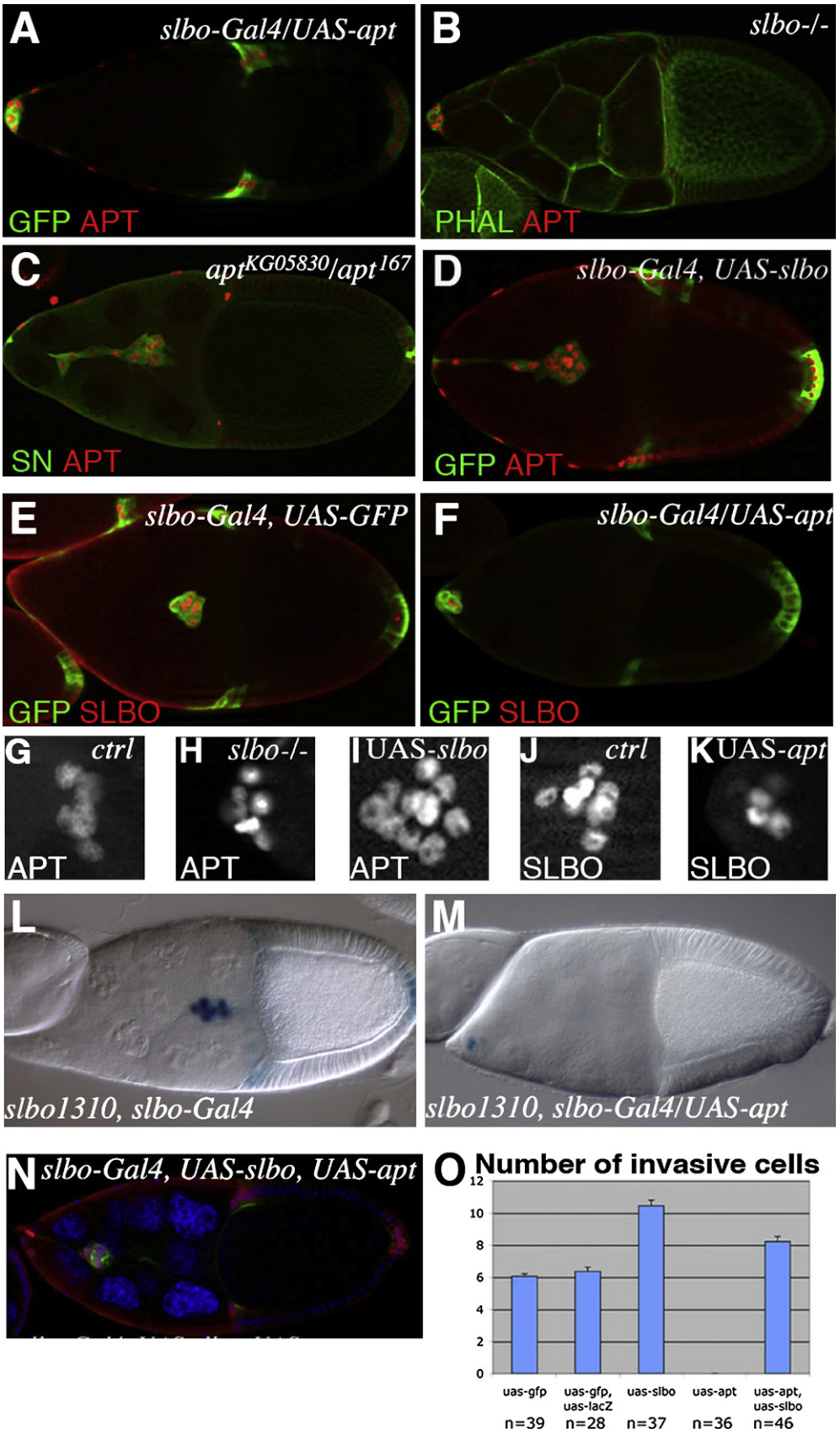
A
slbo-Gal4/UAS-apt
GFP APT
B
slbo-/-
PHAL APT
C
aptKG05830/apt167
SN APT
D
slbo-Gal4, UAS-slbo
GFP APT
E
slbo-Gal4, UAS-GFP
GFP SLBO
F
slbo-Gal4/UAS-apt
GFP SLBO
G
ctrl
APT
H
slbo-/-
APT
I
UAS-slbo
APT
J
ctrl
SLBO
K
UAS-apt
SLBO
L
slbo1310, slbo-Gal4
M
slbo1310, slbo-Gal4/UAS-apt
N
slbo-Gal4, UAS-slbo, UAS-apt
O
Number of invasive cells
12
10
8
6
4
2
0
uas-gfp
uas-gfp, uas-lacZ
uas-slbo
uas-apt
uas-apt, uas-slbo
n=39
n=28
n=37
n=36
n=46

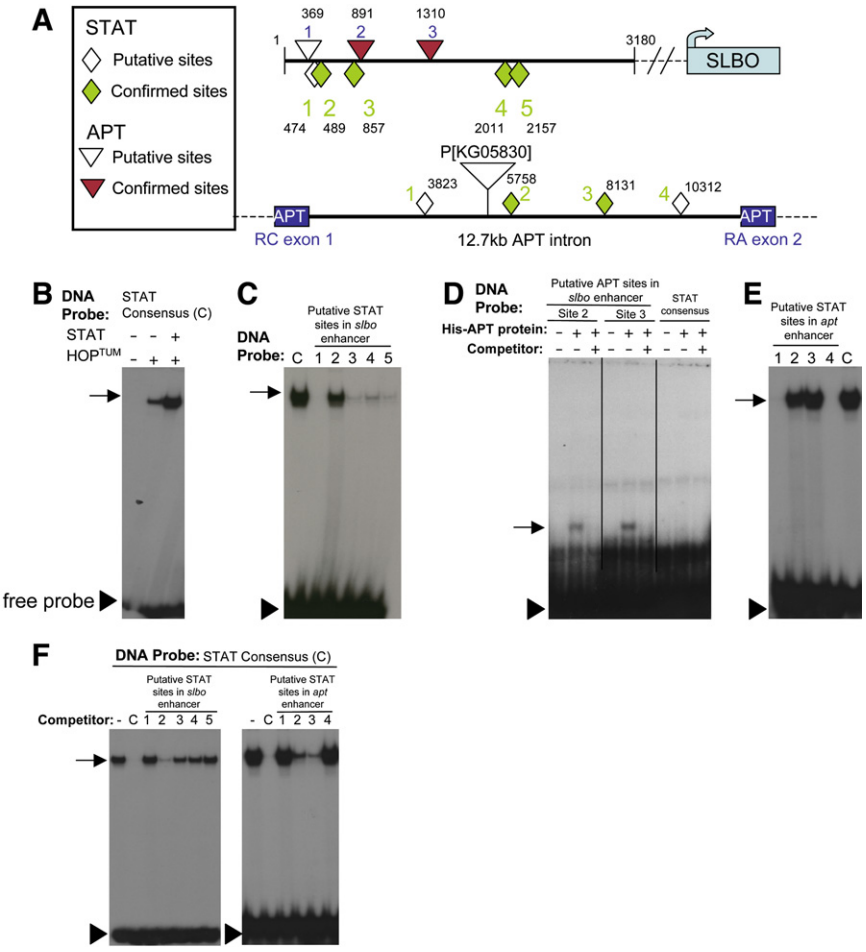

Figure 5. Binding of STAT and APT to *slbo* and *apt* Gene Regulatory Regions

(A) Schematic diagram of putative STAT binding sites (diamonds) and APT binding sites (triangles) in the *slbo* and *apt* gene regulatory regions.

(B–F) EMSAs carried out using S2 cell nuclear extracts ([B], [C], [E], and [F]) or purified His-tagged APT (D). Free probe is indicated by the arrowheads.

(B) Nuclear extracts from control S2 cells or cells overexpressing STAT or co-overexpressing STAT and HOP^{TUM} were incubated with labeled DNA corresponding to the optimal STAT binding consensus sequence C.

(C) Nuclear extracts from S2 cells co-overexpressing STAT and HOP^{TUM} were incubated with labeled oligonucleotides corresponding to predicted STAT binding sites from the *slbo* enhancer (1–5); binding activity is detected for sites 2, 3, 4, and 5. The consensus STAT binding site C was a positive control.

(D) Three putative APT binding sites in the *slbo* enhancer were tested for binding to purified His-tagged APT protein in the absence or presence of cold competitor. APT binding to sites 2 and 3 is shown. The STAT consensus binding site was used as negative control.

(E) Nuclear extracts from S2 cells co-overexpressing STAT and HOP^{TUM} were incubated with labeled DNA probes corresponding to the predicted STAT binding sites from the *apt* intron (1–4). The consensus STAT binding site C was used as a positive control.

(F) Each predicted STAT binding sites from the *slbo* (1–5) and *apt* (1–4) regulatory sequences was tested for the ability to compete binding of labeled consensus STAT binding sequence. No competitor (–) was the negative control. Cold STAT consensus C was the positive control. The specific band shifts are indicated by arrows.

consensus STAT binding site, and carried out electrophoretic mobility shift assays (EMSAs) using S2 cell nuclear extracts. Normal S2 cell extracts did not contain detectable DNA binding activity for the consensus STAT site (Figure 5B). However, nuclear extracts from S2 cells overexpressing STAT did exhibit such an activity, which was further augmented by co-overexpression of HOP^{TUM} together with STAT (Figure 5B).

We then carried out EMSA using the putative STAT binding sites from the *slbo* enhancer. Nuclear extracts from S2 cells co-overexpressing STAT and HOP^{TUM} contained an activity that bound four of the five sites in the *slbo* enhancer (Figure 5C); however, there were clear differences between them. Putative site 2 produced the strongest band shift whereas sites 3, 4, and 5 interacted more weakly. We did not detect any binding to putative site 1.

APT could antagonize SLBO expression either by preventing STAT binding to DNA or by binding to the target enhancer independently. To distinguish between these possibilities, we tested whether the addition of purified APT protein inhibited STAT binding to its consensus site. We did not detect any inhibition of STAT

Figure 4. Antagonistic Relationship between *apt* and *slbo*

(A and B) The border cells fail to initiate migration and remain at the anterior tip of egg chambers overexpressing *apt* (A) or carrying a viable combination of *slbo* alleles (*LY6/e7b*) (B). Border cells are marked with antibodies against APT (red) and GFP (green, [A]) or rhodamine-phalloidin (green, [B]).

(C and D) Stretched border cells are revealed in *apt* mutant egg chambers, stained for APT and SN (C), and in egg chambers where *slbo* is overexpressed, stained for APT and GFP (D).

(E and F) Egg chambers stained with anti-SLBO antibody (red) and anti-GFP (green) to mark the border cells in the control *slbo-Gal4, UAS-mCD8GFP* (E) and in the *slbo-Gal4/UAS-apt; UAS-mCD8GFP* genotype (F).

(G–K) High magnification views of border cell clusters from (A and B) and (D–F). In wild-type (G), note uniform APT staining of all nuclei. In *slbo* mutants (H), the border cells have more APT than the central polar cells. In *slbo*-GAL4/UAS-*slbo* (I), the border cells have less APT than the polar cells. High levels of SLBO are detected in border cells and polar cells in *slbo-Gal4, UAS-mCD8GFP* (J). The polar cells have the highest levels of SLBO in *slbo-Gal4/UAS-apt* (K). Note the decrease in SLBO staining intensity in the border cells compared to (J).

(L–M) X-gal staining (blue) in *slbo-Gal4, slbo^{1310}* (L) and *slbo-Gal4, slbo^{1310}/ UAS-apt* (M) egg chambers. In (M), only the polar cells have high β-galactosidase activity.

(N) Co-overexpression of *slbo* and *apt* eliminates stretched border cells and the border cell cluster invades into the nurse cells (compare [N] to [D] and [F]).

(O) Quantification of invasive cells in *slbo*-Gal4 egg chambers combined with the indicated UAS transgenes. Error bars indicate one standard error.

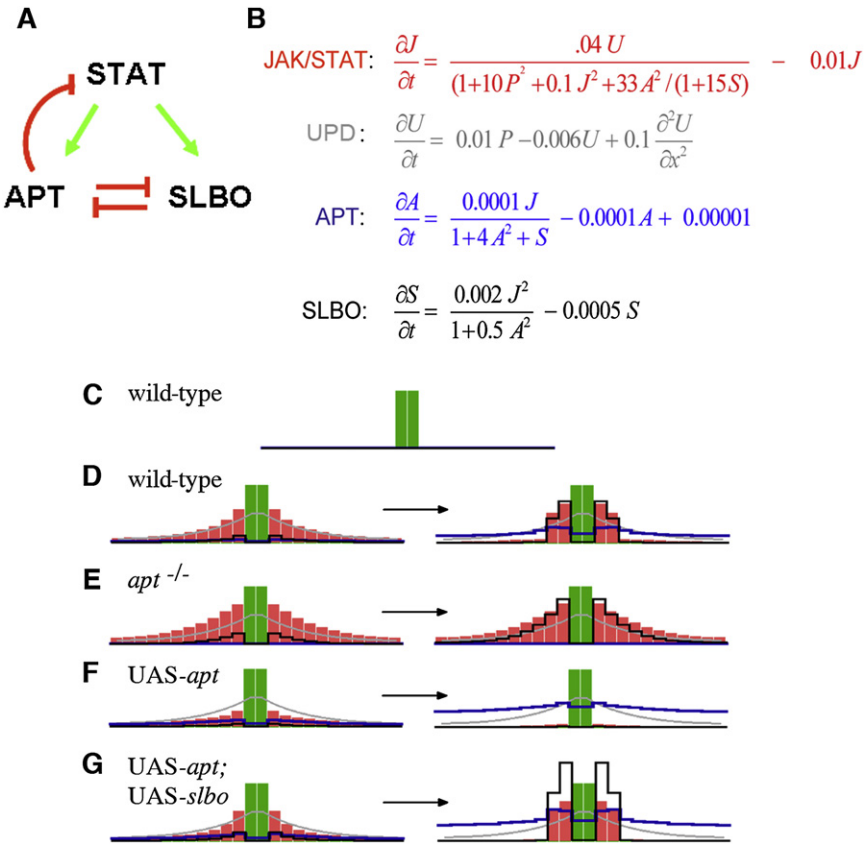

Figure 6. Apontic Limits JAK/STAT Signaling to Determine a Migratory Cell Population

(A) Regulatory circuit indicating the relationships among STAT, APT, and SLBO.

(B) Differential equations describing the changes in the concentration of JAK, UPD, APT, and SLBO over time.

(C–G) A mathematical model simulates border cell specification.

(D–G) An early stage is shown at left; the final steady state at right (after 2,400 and 12,000 iterations, corresponding approximately to the situation at 72 and 360 min).

(C) Initial condition for all simulations: concentrations are zero except for an activator in the two polar cells (green).

(D) In wild-type egg chambers UPD (gray) activates JAK/STAT (red). The latter activates APT (blue) and, especially at higher levels, SLBO (black). APT downregulates JAK/STAT. The mutual suppression of SLBO and APT leads to a switch-like behavior and a step-like JAK/STAT activation, providing an unequivocal signal for border cell specification.

(E) In *apt* mutant egg chambers, JAK/STAT obtains a similar distribution as UPD as the step-like switching component is gone, and the number of migratory cells in increased.

(F) When *apt* production is increased by a factor of three, JAK/STAT did not reach the threshold for *slbo* activation.

(G) When both *apt* and *slbo* are overexpressed (by a factor of three and two, respectively), the stronger suppression of *apt* by SLBO rescues the APT-overexpression phenotype.

binding or a supershift of the STAT/DNA complex by APT (data not shown).

Therefore, we tested whether APT could bind independently of STAT to sites in the *slbo* regulatory region. Although there is no site that perfectly matches the previously identified 14 base pair APT consensus (Liu et al., 2003), we found three sites that contained the central core sequence CCAATT. Histidine-tagged APT protein purified from bacteria (Liu et al., 2003) caused a shift in the electrophoretic mobility of putative sites 2 and 3 (Figure 5D). These interactions were specific as they were competed with excess cold oligonucleotide. APT protein did not shift the STAT consensus oligo, indicating that APT and STAT do not compete for binding to the same site (Figure 5D). We conclude that STAT and APT independently bind directly to distinct sequences within the *slbo* regulatory region.

Since our data indicate that *apt* is also a STAT target, we looked for potential STAT binding sites in the *apt* locus, focusing on the large intron containing the P element insertion that disrupts follicle cell expression specifically. We found four potential sites, which we labeled and incubated with extracts from S2 cells expressing HOP^{TUM} and STAT. STAT bound strongly to sites 2 and 3, but not to site 1 or site 4 (Figure 5E).

To evaluate the binding strengths of each of the identified STAT binding sites from the *slbo* and *apt* genes relative to the STAT consensus site, we carried out competition assays. Equal amounts of cold oligo corresponding to each of the putative STAT binding sites from the *slbo* enhancer or from the *apt* enhancer were used to compete binding of STAT to the labeled optimal STAT binding site. There were clear differences in the ability of the various sequences to compete STAT off of the optimal binding site. Sites 2 and 3 from the *apt* intron were almost as effective as the STAT consensus site itself (Figure 5F). Site 2 from the *slbo* enhancer was also effective (Figure 5F). Sites 3, 4, and 5 from the *slbo* enhancer showed some competition, whereas site 1 did not. These results support the idea that STAT regulates *slbo* and *apt* directly. In addition, the different numbers of binding sites of varying affinities are consistent with the observed differences in the expression patterns of SLBO and APT (see Discussion).

The STAT/APT/SLBO Regulatory Circuit Is Sufficient to Convert a Graded Signal into an "On-Off" Decision

From the genetic and molecular data presented, STAT, APT, and SLBO clearly contribute to patterning the anterior follicular epithelium (Figure 6A). However, it was unclear if these three components would be sufficient to do so. To test this idea, we developed a mathematical model of the regulatory circuit and ran computer simulations of the pattern formation process (Figure 6). The key features of the model are that the levels of active STAT are positively regulated by production of UPD (continuously produced in the polar cells) and negatively regulated by APT. *apt* expression is activated by STAT, whereas APT is inhibited by the STAT-dependent production of SLBO. SLBO expression is activated by STAT and inhibited by APT. In addition, we

incorporated some STAT-independent APT expression, representing the residual APT expression we found in *stat* mutant cells (Figure 3A).

A set of differential equations (Figure 6B) can approximate the relative concentrations of UPD, STAT, APT, and SLBO across the epithelial layer in computer simulations (Figures 6C–6G, Meinhardt, 1982, 2003). Repetition of these computations yielded evolving patterns of gene expression, which accurately reproduced the observed expression of STAT, SLBO, and APT, over the course of a simulated 6 hr period. This was true not only for the wild-type case (Figure 6D), but also for *apt* loss-of-function (Figure 6E) and gain-of-function situations (Figure 6F). Due to the lack of precise kinetic data, the parameters were approximated and adapted in order to reproduce the observed regulatory properties. However, the precise numerical values provided are not critical as long as the balance of APT and SLBO is maintained. The model was further tested by simulating the effect of co-overexpressing SLBO and APT together (Figure 6G). In each situation, the simulation produced the phenotype observed in vivo. This model demonstrates that the regulatory circuit we describe is sufficient to convert an initially broad and graded activation of STAT across a field of cells into a discrete boundary between migratory and stationary cells, and to explain the observed mutant phenotypes.

DISCUSSION

Escape from the Follicular Epithelium

In many migratory cell types, including metastatic carcinomas, motile cells must detach from an epithelium to move to their final location. However the precise mechanisms by which cells disengage from their neighbors remain poorly understood, and in most cases it is not possible to view the process directly in vivo. Border cells in the *Drosophila* ovary represent a model for studying epithelial cell migration in vivo that is amenable both to genetic approaches and live imaging. Here we report the identification of a mutant, *apt*, in which the distinction between invasive and noninvasive cells was compromised. In *apt* mutants, as the border cell cluster moved away from the epithelium, additional migratory cells—the stretched border cells—ingressed in between the nurse cells. These stretched border cells maintained connections with both the main cluster of border cells, and the outer epithelial cell layer, resulting in a defect in detachment.

Recent technological advances have enabled us to analyze border cells throughout their six hour migration by live imaging (Prasad and Montell, 2007). Time-lapse movies of wild-type egg chambers revealed that the process of border cell detachment is surprisingly slow. This indicates that the ability to extend and retract protrusions is not sufficient for the border cells to exit the epithelium, and that there is sufficient time for transcriptional events to contribute to the process. In *apt* mutants, the border cells rounded up and advanced in between the nurse cells normally, but cells with an apparently intermediate identity were frequently trapped in between the border cell cluster and the follicle cell epithelium, unable to detach from either one. Thus, the two cell types must be clearly distinguished in order for them to be able to disconnect from one another.

A Simple Gene Regulatory Circuit Converts the Graded JAK/STAT Signal into "On" and "Off" States, Delimiting the Migratory Border Cell Population

In a variety of contexts throughout development, a graded distribution of a signaling molecule in a field of cells can elicit discrete cellular responses. Such threshold-like behavior can be achieved by positive autoregulation (Meinhardt, 1982, 2003), which is a property of the JAK/STAT pathway (Arbouzova and Zeidler, 2006; Harrison et al., 1998). Therefore, prior to the current work, it would have been reasonable to propose that STAT autoregulation could convert initially graded activity in the follicular epithelium to "on" and "off" states. In wild-type, the migrating border cell cluster takes the source of JAK/STAT activation (UPD expressed by the polar cells) with it, reinforcing SLBO expression in the migratory cells and removing the source of JAK/STAT activation from the anterior follicle cells. So, one could have postulated that the physical separation of the JAK/STAT signaling center from the anterior follicle cells was sufficient to create a significant difference in levels of STAT activity between the migrating cells and those left behind, and thus to distinguish the two cell types and behaviors. However, unexpectedly we show that neither STAT autoregulation nor the movement of the signaling center is sufficient to convert the gradient into a step function in the absence of APT.

We propose instead that feedback inhibition of JAK/STAT combined with the mutual repression of APT and SLBO is responsible for generating the stepwise activation pattern. When two genes mutually repress each other, a slight increase in the activation of one leads to a stronger repression of the second, which, in turn, leads to a further increase of the first. Thus, together these two genes behave as an autocatalytic system (Meinhardt, 1982). Since *apt* and *slbo* are both targets of STAT activity, we propose a three-component regulatory circuit. Our mathematical model demonstrates that this circuit is sufficient to explain what we observed in vivo. In the absence of APT, JAK/STAT activation takes place in an enlarged region and, remarkably, the "on-off" character of the JAK/STAT activation is lost. This suggests that the threshold behavior of the system does not result from JAK/STAT autoregulation but from the mutual repression of APT and SLBO.

The model that most accurately simulates the wild-type and mutant phenotypes is one in which SLBO antagonizes APT activity more strongly than its expression. This is consistent with our experimental observation that overexpression of SLBO completely mimics the *apt* loss-of-function phenotype, but only reduces and does not eliminate APT expression (Figure 4).

It is striking that different patterns of SLBO and APT are induced by the same gradient of JAK/STAT activity. An important consequence is that, at high concentrations of active STAT, more SLBO is produced than APT. One way this could be explained is through our observation that STAT bound four different sites in the *slbo* enhancer with differing affinities. In cells with high concentrations of STAT, more sites, including low affinity sites, should be occupied and thus a higher level of *slbo* expression generated than in cells with lower STAT levels. In contrast, the *apt* gene contains only two detectable STAT binding sites, to which STAT can bind nearly as well as it binds the optimal STAT consensus sequence. Thus, *apt* expression should turn on in response to lower levels of active STAT than *slbo* and

also should saturate at relatively low concentrations of active STAT, yielding a broad and shallow expression gradient across the anterior field of follicle cells. These are precisely the expression patterns observed. Therefore, in cells adjacent to the polar cells, SLBO wins the competition whereas further away from the source of UPD, APT wins the APT/SLBO competition. Higher levels of SLBO block the repression of JAK/STAT by APT in the cells next to the polar cells, causing an even stronger JAK/STAT activation and so on.

In addition, we found evidence for a low level of JAK/STAT-independent APT expression, which we also incorporated into the model. This baseline APT expression depended on the transcription factor known as Eyes Absent (data not shown), and based on the model we propose that its function could be to prevent any possibility of a renewed trigger of the JAK/STAT pathway in the cells that remain in the anterior epithelium.

A Conserved Role for APT in the JAK/STAT Pathway?

The JAK/STAT pathway is highly conserved from insects to mammals and is critically important in development, immunity, and inflammation. Intriguingly, *Drosophila* APT is expressed in many domains where JAK/STAT signaling occurs, including embryonic trachea and the hub of the testes (data not shown and [Brown et al., 2001; Chen et al., 2002; Li et al., 2003]). In addition, *apt* has been uncovered as a downstream target of STAT in microarray analysis of testis (Terry et al., 2006) and border cells (X.W. and D.J.M., unpublished data). Therefore, *apt* may be a downstream target of STAT signaling in a variety of cell types.

It is also possible that this relationship is conserved in other animals, as genes highly related to *apt* are found in all sequenced insect genomes. In humans, the closest gene to *apt* is *fibrinogen silencer-binding protein (FSBP*). Interestingly, two strong loss-of-function alleles of *apt* contain missense mutations in well-conserved residues, demonstrating the functional significance of this region. Although FSBP has not been extensively characterized, it has been reported to be a negative regulator of the gamma chain of *fibrinogen* transcription (Mizuguchi et al., 1995). Fibrinogen is highly expressed in hepatocytes in response to inflammatory cytokine-mediated activation of the JAK/STAT pathway, and there are at least three STAT3 binding sites on the human *gamma-fibrinogen* promoter (Duan and Simpson-Haidaris, 2003). This suggests that APT and FSBP could fulfill similar functions as negative regulators of STAT-responsive genes.

All of the major growth factor and cytokine signaling pathways are subject to extensive positive and negative feedback regulation, which is crucial to generate appropriate physiological responses (reviewed in Freeman, 2000). The work presented here establishes APT as a feedback inhibitor of JAK/STAT signaling and cell invasion.

EXPERIMENTAL PROCEDURES

Screen for Border Cell Migration Mutants

We obtained from the Bloomington Stock Center 2951 homozygous-viable P element insertion lines, generated in the P element Disruption Project (Bellen et al., 2004). Females were fattened on yeasted vials overnight at room temperature; their ovaries were dissected into 96-well dishes. Antibody staining was carried out as previously described (McDonald et al., 2006) with mouse anti-ARM (1:50, N27A1, Iowa Developmental Studies Hybridoma Bank, DSHB), followed by DAPI and secondary antibody treatment (1:400, anti-mouse Alexa 488, Molecular Probes). Ovaries were mounted in 70% glycerol on slides and scored for cell migration phenotypes. Lines displaying migration defects in more than 10% of egg chambers were kept for secondary screening. Images were obtained using a Zeiss Axioplan Apotome microscope using AxioVision software. Some images were processed in Adobe Photoshop.

Characterization of a Novel *apontic* Allele

The Gene Disruption Project mapped P{SUPor-P}^{KG05830} to the first intron of *apontic* at 2R:19460785. Using primers flanking this location (Integrated DNA Technologies, IDT) and P element primers, we confirmed this location. For expression and complementation tests, we used the following strains (Bloomington Stock Center): y[1] w[67c23]; P{w[+mC] = lacW}apt[k15608]/CyO, cn[1] P{ry[+t7.2] = PZ}apt[03041]/CyO; ry[506], Df(2R)Exel7180, (Df(2R)egl3 complemented). *apt*^{41} and *apt*^{167} were gifts from W. McGinnis; *apt*$^{tdfP\Delta 3}$, *apt* $^{tdfP\Delta 4}$, *apt* $^{tdfC5\text{-}2\text{-}5}$, and the *UAS-tdf* line were gifts of R. Schuh. Mosaic analysis and MARCM positively marked clonal experiments were carried out as described (Lee and Luo, 1999; Liu and Montell, 1999).

Rabbit or rat anti-Apontic antibodies were gifts of R. Schuh, P. Macdonald, and S. Hirose. Mouse anti-Singed (c7sn, 1:25), rat anti-E-cadherin (E-cad1, 1:25), mouse anti-ARM (1:50), and mouse anti-EYA (1:50) came from the DSHB. P. Rorth provided rat anti-SLBO antibody (1:1000). Rabbit anti-STAT (1:800) was generated against a peptide designed by S. Hou. Border cell/stretch border cells were counted by staining for DAPI, anti-ARM, and anti-EYA.

β-Galactosidase Activity

β-Galactosidase activity was detected as previously described (Liu and Montell, 1999). Ovaries were dissected in Schneider's media with 10% FBS, fixed in 4% formaldehyde, washed, and stained with 0.2% X-Gal staining solution until signal was detected (4–6 hr). For comparisons, each sample was developed for the same amount of time.

Bioinformatics

Apontic and Fibrinogen Silencer-Binding Protein sequences were obtained from The National Center for Biotechnology Information (http://www.ncbi.nlm.nih.gov). Sequence alignment was performed using ClustalW (http://www.ebi.ac.uk/clustalw/). Coiled-coil domains were predicted using http://npsa-pbil.ibcp.fr.

Overexpression Experiments

For overexpression experiments, the following genotypes were used: *slbo*-Gal4 (Rorth, 1994); or *slbo*-Gal4, UAS-mCD8-GFP; or *slbo*^{1310}, *slbo*-Gal4; UAS-*tdf* (Eulenberg and Schuh, 1997), UAS-*LacZ* or UAS-mCD8-GFP, UAS-DOME$^{\Delta CYT}$ (Brown et al., 2001), UAS-Hop^{Tum} (Harrison et al., 1995), UAS-Slbo (Rorth et al., 2000). Flies were fattened overnight at 31°C. To measure levels of APT protein, images of antibody staining were obtained, positive nuclei were outlined in Axiovision, and pixel intensity was measured.

Live Imaging

Live imaging experiments were performed as described (Prasad and Montell, 2007). Images were acquired every 3 min for up to 6 hr. The wild-type control genotype was *slbo*-Gal4, UAS-mCD8-GFP. For *apt* imaging, the genotype was *slbo*-Gal4, *apt*^{KG05830}/UAS-mCD8-GFP, *apt*^{167}. For overexpression of SLBO experiments, the genotype was *slbo*-Gal4, UAS-*slbo*; UAS-mCD8-GFP. Flies were fattened on yeasted vials at 31° overnight, and moved to room temperature for 4 hr before being dissected.

Other Fly Genetics

To activate the STAT pathway in different cell types, we expressed a constitutively active JAK (*hop*^{Tum}) in random clones of cells using the FLP-out method as described (Ito et al., 1997). Flies were heat shocked for 30 min, rested for 1 d, and then fattened and dissected the next day. To analyze APT in the *slbo* mutant background, the *slbo*^{e7b}/*slbo*^{LY6} alleles were used. *stat*^{1681} was used to test for genetic interactions with *apt*^{KG05830}/*apt*^{167}. Invasive cell numbers were determined by staining for DAPI, Anti-ARM, and a cell's location within the nurse cell cluster.

Electrophoretic Mobility Shift Assay, EMSA

To identify putative STAT binding sites in *slbo* and *apt* regulatory regions, we used Transfac software (http://www.genomatix.de/cgi-bin/gems/launch.pl). We chose a statistically calculated maximal STAT binding site (consensus STAT) as a positive control. Sequences of the 25 bp oligonucleotides containing the various binding sites are in the Supplemental Data. Nuclear extracts were prepared as described (Sovak et al., 1997), from *Drosophila* S2 untransfected cells, or those transfected with pMT-v5-STAT or pMT-v5-STAT and act-HOP^{TUM} (gifts of M. Zeidler) using the QIAGEN Effectine kit. To induce STAT expression, 1mM of $CuSO_4$ was added after 24 hr. For the binding reaction, 5 μg of nuclear extract was used and DNA-protein complexes were separated as described (Sovak et al., 1997). For competition assays, 50-fold excess unlabeled oligonucleotide was incubated with nuclear extracts for 30 min at room temperature prior to addition of the probe. His-APT DNA was a gift of S. Hirose. Protein was purified using QIAGEN NTA Ni-Agarose Fast Start Kit. For APT binding, EMSAs were carried out as described (Ueda and Hirose, 1991), except electrophoresis was carried out on 6% 0.5X TBE gels.

SUPPLEMENTAL DATA

Supplemental Data include three figures, Supplemental Experimental Procedures, and four movies and can be found with this article online at http://www.developmentalcell.com/cgi/content/full/14/5/726/DC1/.

ACKNOWLEDGMENTS

We thank members of the fly community for reagents, as listed in the text. We acknowledge Tanika Harris, Tina Bridges, and Stacey Bridges for technical assistance. We thank current and past members of the Montell Lab and Craig Montell for helpful comments and discussion. Thanks to Jonathan Pevsner for his collaboration with the bioinformatics analysis of *apontic* and related sequences. M.S.G. was supported by a fellowship from the American Cancer Society. NIH grants GM46425 and GM73164 to D.J.M. supported this work.

Received: July 24, 2007
Revised: January 25, 2008
Accepted: March 10, 2008
Published: May 12, 2008

REFERENCES

Arbouzova, N.I., and Zeidler, M.P. (2006). JAK/STAT signalling in *Drosophila*: insights into conserved regulatory and cellular functions. Development *133*, 2605–2616.

Bach, E.A., Ekas, L.A., Ayala-Camargo, A., Flaherty, M.S., Lee, H., Perrimon, N., and Baeg, G.H. (2007). GFP reporters detect the activation of the *Drosophila* JAK/STAT pathway in vivo. Gene Expr. Patterns *7*, 323–331.

Beccari, S., Teixeira, L., and Rorth, P. (2002). The JAK/STAT pathway is required for border cell migration during *Drosophila* oogenesis. Mech. Dev. *111*, 115–123.

Bellen, H.J., Levis, R.W., Liao, G., He, Y., Carlson, J.W., Tsang, G., Evans-Holm, M., Hiesinger, P.R., Schulze, K.L., Rubin, G.M., et al. (2004). The BDGP gene disruption project: single transposon insertions associated with 40% of *Drosophila* genes. Genetics *167*, 761–781.

Brown, S., Hu, N., and Hombria, J.C. (2001). Identification of the first invertebrate interleukin JAK/STAT receptor, the *Drosophila* gene domeless. Curr. Biol. *11*, 1700–1705.

Chen, H.W., Chen, X., Oh, S.W., Marinissen, M.J., Gutkind, J.S., and Hou, S.X. (2002). mom identifies a receptor for the *Drosophila* JAK/STAT signal transduction pathway and encodes a protein distantly related to the mammalian cytokine receptor family. Genes Dev. *16*, 388–398.

Devergne, O., Ghiglione, C., and Noselli, S. (2007). The endocytic control of JAK/STAT signalling in *Drosophila*. J. Cell Sci. *120*, 3457–3464.

Duan, H.O., and Simpson-Haidaris, P.J. (2003). Functional analysis of interleukin 6 response elements (IL-6REs) on the human γ-fibrinogen promoter: binding of hepatic Stat3 correlates negatively with transactivation potential of type II IL-6REs. J. Biol. Chem. *278*, 41270–41281.

Eulenberg, K.G., and Schuh, R. (1997). The tracheae defective gene encodes a bZIP protein that controls tracheal cell movement during *Drosophila* embryogenesis. EMBO J. *16*, 7156–7165.

Freeman, M. (2000). Feedback control of intercellular signalling in development. Nature *408*, 313–319.

Fulga, T.A., and Rorth, P. (2002). Invasive cell migration is initiated by guided growth of long cellular extensions. Nat. Cell Biol. *4*, 715–719.

Geisbrecht, E.R., and Montell, D.J. (2002). Myosin VI is required for E-cadherin-mediated border cell migration. Nat. Cell Biol. *4*, 616–620.

Gellon, G., Harding, K.W., McGinnis, N., Martin, M.M., and McGinnis, W. (1997). A genetic screen for modifiers of Deformed homeotic function identifies novel genes required for head development. Development *124*, 3321–3331.

Ghiglione, C., Devergne, O., Georgenthum, E., Carballes, F., Medioni, C., Cerezo, D., and Noselli, S. (2002). The *Drosophila* cytokine receptor Domeless controls border cell migration and epithelial polarization during oogenesis. Development *129*, 5437–5447.

Harrison, D.A., Binari, R., Nahreini, T.S., Gilman, M., and Perrimon, N. (1995). Activation of a *Drosophila* Janus kinase (JAK) causes hematopoietic neoplasia and developmental defects. EMBO J. *14*, 2857–2865.

Harrison, D.A., McCoon, P.E., Binari, R., Gilman, M., and Perrimon, N. (1998). *Drosophila* unpaired encodes a secreted protein that activates the JAK signaling pathway. Genes Dev. *12*, 3252–3263.

Ito, K., Awano, W., Suzuki, K., Hiromi, Y., and Yamamoto, D. (1997). The *Drosophila* mushroom body is a quadruple structure of clonal units each of which contains a virtually identical set of neurones and glial cells. Development *124*, 761–771.

Jang, A.C., Starz-Gaiano, M., and Montell, D.J. (2007). Modeling migration and metastasis in Drosophila. J. Mammary Gland Biol. Neoplasia *12*, 103–114.

King, R.C. (1970). Ovarian Development in *Drosophila melanogaster* (New York: Academic Press).

Lee, T., and Luo, L. (1999). Mosaic analysis with a repressible cell marker for studies of gene function in neuronal morphogenesis. Neuron *22*, 451–461.

Li, J., Li, W., Calhoun, H.C., Xia, F., Gao, F.B., and Li, W.X. (2003). Patterns and functions of STAT activation during *Drosophila* embryogenesis. Mech. Dev. *120*, 1455–1468.

Lie, Y.S., and Macdonald, P.M. (1999). Apontic binds the translational repressor Bruno and is implicated in regulation of oskar mRNA translation. Development *126*, 1129–1138.

Liu, Q.X., Jindra, M., Ueda, H., Hiromi, Y., and Hirose, S. (2003). *Drosophila* MBF1 is a co-activator for Tracheae Defective and contributes to the formation of tracheal and nervous systems. Development *130*, 719–728.

Liu, Y., and Montell, D.J. (1999). Identification of mutations that cause cell migration defects in mosaic clones. Development *126*, 1869–1878.

McDonald, J.A., Pinheiro, E.M., Kadlec, L., Schupbach, T., and Montell, D.J. (2006). Multiple EGFR ligands participate in guiding migrating border cells. Dev. Biol. *296*, 94–103.

Meinhardt, H. (1982). Theory of regulatory functions of the genes in the bithorax complex. Prog. Clin. Biol. Res. *85*, 337–348.

Meinhardt, H. (2003). Complex pattern formation by a self-destabilization of established patterns: chemotactic orientation and phyllotaxis as examples. C. R. Biol. *326*, 223–237.

Mizuguchi, J., Hu, C.H., Cao, Z., Loeb, K.R., Chung, D.W., and Davie, E.W. (1995). Characterization of the 5′-flanking region of the gene for the gamma chain of human fibrinogen. J. Biol. Chem. *270*, 28350–28356.

Montell, D.J. (2006). The social lives of migrating cells in *Drosophila*. Curr. Opin. Genet. Dev. *16*, 374–383.

Montell, D.J., Rorth, P., and Spradling, A.C. (1992). slow border cells, a locus required for a developmentally regulated cell migration during oogenesis, encodes *Drosophila* C/EBP. Cell *71*, 51–62.

Prasad, M., and Montell, D.J. (2007). Cellular and molecular mechanisms of border cell migration analyzed using time-lapse live-cell imaging. Dev. Cell *12*, 997–1005.

Rorth, P. (1994). Specification of C/EBP function during *Drosophila* development by the bZIP basic region. Science *266*, 1878–1881.

Rorth, P., Szabo, K., and Texido, G. (2000). The level of C/EBP protein is critical for cell migration during *Drosophila* oogenesis and is tightly controlled by regulated degradation. Mol. Cell *6*, 23–30.

Silver, D.L., and Montell, D.J. (2001). Paracrine signaling through the JAK/STAT pathway activates invasive behavior of ovarian epithelial cells in *Drosophila*. Cell *107*, 831–841.

Silver, D.L., Geisbrecht, E.R., and Montell, D.J. (2005). Requirement for JAK/STAT signaling throughout border cell migration in *Drosophila*. Development *132*, 3483–3492.

Sovak, M.A., Bellas, R.E., Kim, D.W., Zanieski, G.J., Rogers, A.E., Traish, A.M., and Sonenshein, G.E. (1997). Aberrant nuclear factor-κB/Rel expression and the pathogenesis of breast cancer. J. Clin. Invest. *100*, 2952–2960.

Su, M.T., Venkatesh, T.V., Wu, X., Golden, K., and Bodmer, R. (1999). The pioneer gene, apontic, is required for morphogenesis and function of the *Drosophila* heart. Mech. Dev. *80*, 125–132.

Terry, N.A., Tulina, N., Matunis, E., and DiNardo, S. (2006). Novel regulators revealed by profiling *Drosophila* testis stem cells within their niche. Dev. Biol. *294*, 246–257.

Ueda, H., and Hirose, S. (1991). Defining the sequence recognized with BmFTZ-F1, a sequence specific DNA binding factor in the silkworm, *Bombyx mori*, as revealed by direct sequencing of bound oligonucleotides and gel mobility shift competition analysis. Nucleic Acids Res. *19*, 3689–3693.

Xi, R., McGregor, J.R., and Harrison, D.A. (2003). A gradient of JAK pathway activity patterns the anterior-posterior axis of the follicular epithelium. Dev. Cell *4*, 167–177.